



Dynamically generated 1^+ heavy mesons

Feng-Kun Guo^{a,b,f,*}, Peng-Nian Shen^{a,b,d,e}, Huan-Ching Chiang^{a,c}

^a Institute of High Energy Physics, Chinese Academy of Sciences, PO Box 918(4), Beijing 100049, China

^b CCAST (World Laboratory), PO Box 8730, Beijing 100080, China

^c South-West University, Chongqing 400715, China

^d Institute of Theoretical Physics, Chinese Academy of Sciences, PO Box 2735, China

^e Center of Theoretical Nuclear Physics, National Laboratory of Heavy Ion Accelerator, Lanzhou 730000, China

^f Graduate University of Chinese Academy of Sciences, Beijing 100049, China

Received 9 October 2006; received in revised form 31 December 2006; accepted 23 January 2007

Available online 20 February 2007

Editor: J.-P. Blaizot

Abstract

By using a heavy chiral unitary approach, we study the S wave interactions between heavy vector meson and light pseudoscalar meson. By searching for poles of the unitary scattering amplitudes in the appropriate Riemann sheets, several 1^+ heavy states are found. In particular, a D^*K bound state with a mass of 2.462 ± 0.010 GeV which should be associated with the recently observed $D_{s1}(2460)$ state is obtained. In the same way, a $B^*\bar{K}$ bound state (B_{s1}) with mass of 5.778 ± 0.007 GeV in the bottom sector is predicted. The spectra of the dynamically generated D_1 and B_1 states in the $I = 1/2$ channel are also calculated. One broad state and one narrow state are found in both the charmed and bottom sectors. The coupling constants and decay widths of the predicted states are further investigated.

© 2007 Elsevier B.V. Open access under [CC BY license](http://creativecommons.org/licenses/by/3.0/).

PACS: 14.40.Lb; 12.39.Fe; 13.75.Lb; 13.25.Ft

Keywords: $D_{s1}(2460)$; Heavy chiral unitary approach; Dynamically generated states

1. Introduction

In recent years, the discovery of various new hadron states stimulated much theoretical effort on the hadron spectrum. Among these states, $D_{s0}^*(2317)$ and $D_{s1}(2460)$ [1] are the most attractive ones, because the measured masses are smaller than those predicted in terms of most phenomenological models [2] (refer to the recent review articles [3]). Many physicists presumed that these new states are conventional $c\bar{s}$ mesons [2,4], and the others believed that they might be exotic meson states, such as tetraquark states [5], molecular states [6–9], or admixture of $c\bar{s}$ with molecular component or tetraquark component [10], and etc.

In the corresponding non-strange sector, there are two confirmed D_1 states. The narrow one is named as $D_1(2420)$

with mass of 2423.4 ± 3.1 MeV and width of 25 ± 6 MeV, and the broad one is entitled as $D_1(2430)$ with mass of $2427 \pm 26 \pm 25$ MeV and width of $384_{-75}^{+107} \pm 74$ MeV [11,12]. Theoretically, the wide-width state with mass of 2325 MeV and narrow-width state with mass of 2552 MeV were declared in the χ -SU(3) approach [7]. In Ref. [8], these two states were considered as quasi-bound states and were used to determine the unknown coupling constants in the next-to-leading order heavy chiral Lagrangian. The reproduced masses and widths are $M_{D_1} = 2422$ MeV and $\Gamma_{D_1} = 23$ MeV and $M_{D_1'} = 2300$ MeV and $\Gamma_{D_1'} = 300$ MeV, respectively. In many other references [13–17], these two states were proposed as the conventional $c\bar{q}$ states, for instance, in Ref. [15], they were deliberated as the mixed 1P_1 and $^3P_1c\bar{q}$ states with a mixing angle of $\phi \approx 35^\circ$ obtained by fitting measured widths.

Since the $D_{s0}^*(2317)$ and $D_{s1}^*(2460)$ have the same quantum number I , the isospin, and S , the strangeness, except J , the total angular momentum, in the S wave DK and D^*K chan-

* Corresponding author at: Institute of High Energy Physics, Chinese Academy of Sciences, PO Box 918(4), Beijing 100049, China.

E-mail address: guofk@mail.ihep.ac.cn (F.-K. Guo).

nels, respectively, it would be constructive to study the DK and D^*K interactions so that one can see whether these two states could have similar molecular structure. In the light hadron system, the chiral unitary approach (ChUA) has achieved great success in explaining the meson–meson and meson–baryon interactions [18–25]. Some well-known hadrons can be dynamically generated as the quasi-bound states of two mesons or a meson and a baryon [24], for instance, the lowest scalar states σ , $f_0(980)$, $a_0(980)$, κ [19–21,25], and etc. Then, the approach was extended to the heavy hadron system, called heavy chiral unitary approach (HChUA) [26]. In terms of such an approach, the S wave interaction between the heavy meson and light pseudoscalar meson was studied, and some bound states and resonances were predicted, for example, the D_{s0}^* (2317) state as a DK bound state at 2.312 ± 0.041 GeV, a $B\bar{K}$ bound state at 5.725 ± 0.039 GeV [26]. In the same approach, D_0^* and B_0^* in the $(I, S) = (1/2, 0)$ channel were also investigated. As a result, one broad state and one narrow state were predicted in both the charmed and bottom sectors [26].

In this Letter, we study the S wave interaction between heavy vector meson and light pseudoscalar meson and search for $J^P = 1^+$ heavy mesons in both strange and non-strange sectors. The couplings of various coupled channels to the generated states and the decay width of the isospin symmetry violating process $D_{s1}(2460)^+ \rightarrow D_s^{*+}\pi^0$ are studied as well.

2. Dynamically generated heavy–light 1^+ states

To describe the interaction between the heavy vector meson and the light pseudoscalar meson, we employ a leading order heavy chiral Lagrangian [7,27]

$$\mathcal{L} = -\frac{1}{4f_\pi^2} (\partial^\mu P^{*\nu} [\Phi, \partial_\mu \Phi] P_\nu^{*\dagger} - P^{*\nu} [\Phi, \partial_\mu \Phi] \partial^\mu P_\nu^{*\dagger}), \quad (1)$$

where $f_\pi = 92.4$ MeV is the pion decay constant, P_ν^* represents the heavy vector mesons with quark contents $(Q\bar{u}, Q\bar{d}, Q\bar{s})$, namely $(D^{*0}, D^{*+}, D_s^{*+})$ and $(B^{*-}, \bar{B}^{*0}, \bar{B}_s^*)$ for the charmed and bottom sectors, respectively, and Φ denotes the octet Goldstone bosons in the 3×3 matrix form

$$\Phi = \begin{pmatrix} \frac{1}{\sqrt{2}}\pi^0 + \frac{1}{\sqrt{6}}\eta & \pi^+ & K^+ \\ \pi^- & -\frac{1}{\sqrt{2}}\pi^0 + \frac{1}{\sqrt{6}}\eta & K^0 \\ K^- & \bar{K}^0 & -\frac{2}{\sqrt{6}}\eta \end{pmatrix}. \quad (2)$$

We are interested in $(I, S) = (0, 1)$ and $(I, S) = (1/2, 0)$ systems. Usually, such a system can be characterized by its own isospin. Based on the Lagrangian in Eq. (1), the amplitude with a definite isospin can be written as

$$V_{ij}^I(s, t, u)\varepsilon \cdot \varepsilon' = -\frac{C_{ij}^I}{4f_\pi^2}(s-u)\varepsilon \cdot \varepsilon', \quad (3)$$

where i and j denote the initial state and the final state, respectively, s, t, u are usual Mandelstam variables, and ε and ε' are polarization vectors of the vector states in the initial and final states, respectively. In the $I = 0$ case, there are two coupled channels. The channel labels $i = 1$ and 2 specify the D^*K

Table 1
Coefficients C_{ij}^I in Eq. (3)

| C_{11}^0 | C_{12}^0 | C_{22}^0 | $C_{11}^{1/2}$ | $C_{12}^{1/2}$ | $C_{22}^{1/2}$ | $C_{13}^{1/2}$ | $C_{23}^{1/2}$ | $C_{33}^{1/2}$ |
|------------|------------|------------|----------------|----------------|----------------|-----------------------|-----------------------|----------------|
| -2 | $\sqrt{3}$ | 0 | -2 | 0 | 0 | $-\frac{\sqrt{6}}{2}$ | $-\frac{\sqrt{6}}{2}$ | -1 |

($B^*\bar{K}$) and $D_s^*\eta$ ($B_s^*\eta$) channels in the charmed (bottom) sector, respectively. In the $I = 1/2$ case, three coupled channels exist. The channel labels $i = 1, 2$ and 3 in this case denote the $D^*\pi$ ($B^*\pi$), $D^*\eta$ ($B^*\eta$) and $D_s^*\bar{K}$ (B_s^*K) in the charmed (bottom) sector, respectively. The corresponding coefficients C_{ij}^I are tabulated in Table 1. It should be mentioned that, in the coupled channel calculation, the thresholds of the channels with the light vector meson and the heavy pseudoscalar one are relatively higher than those with the light pseudoscalar meson and the heavy vector one. For instance, in the charmed $I = 1/2$ case, the lightest combination of a light vector meson and heavy pseudoscalar meson is $\rho + D$, and the sum of their masses are almost forty MeV heavier than that of the heaviest combination of a light pseudoscalar meson and heavy vector meson, say $K + D_s^*$. Thus, in the concerned energy region near the thresholds of the channels with later combinations, the contributions from the channels with former combinations are expected to be less important, and hence can be neglected for simplicity.

In ChUA, the unitary scattering amplitude can be expressed by the algebraic Bethe–Salpeter equation [19]. The full unitary amplitude for the S wave scattering of vector and light pseudoscalar mesons can be written as [7,24]

$$T^I(s) = -\left[1 + V^I(s)G(s)\left(1 + \frac{q_{\text{on}}^2}{3M_V^2}\right)\right]^{-1} V^I(s), \quad (4)$$

where the polarization vectors are dropped because they are irrelevant to the pole searching. In the equation, M_V is the mass of the vector meson in the meson loop and q_{on} represents the on-shell three-momentum in the center of mass frame. $V^I(s)$ is in the matrix form with its elements being the S wave projections of $V_{ij}^I(s, t, u)$. The non-zero element of the diagonal matrix $G(s)$ is the two-meson loop integral

$$G_{ii}(s) = i \int \frac{d^4q}{(2\pi)^4} \frac{1}{q^2 - m_\phi^2 + i\varepsilon} \frac{1}{(p_1 + p_2 - q)^2 - M_V^2 + i\varepsilon}, \quad (5)$$

where m_ϕ is the mass of the light pseudoscalar meson in the loop. The loop integral is calculated in terms of the dispersion relation with a pre-selected subtraction constant $a(\mu)$ [21]. The subtraction constant can be fixed by matching the calculated loop integral with that calculated by using the three-momentum cut-off method [26]. The matching point is taken at $M_{D^*} + m_K$ for the charmed sector and $M_{B^*} + m_K$ for the bottom sector, respectively, because we are interested in the energy region around the threshold. With the same consideration shown in Ref. [26], the estimated three-momentum cutoff q_{max} is in the region of 0.8 ± 0.2 GeV. The corresponding values of $a(\mu)$ and q_{max} are tabulated in Table 2. The resultant loop integration curves in two different methods are plotted in Fig. 1. It is shown that they are very similar with each other in the region

Table 2

Corresponding $a(\mu)$ values and q_{\max} values with $\mu = m_D$ for the charmed sector and $\mu = m_B$ for the bottom sector, respectively

| q_{\max} (GeV) | 0.6 | 0.8 | 1.0 |
|------------------|---------|--------|--------|
| $a(m_D)$ | -0.639 | -0.714 | -0.752 |
| $a(m_B)$ | -0.0764 | -0.101 | -0.113 |

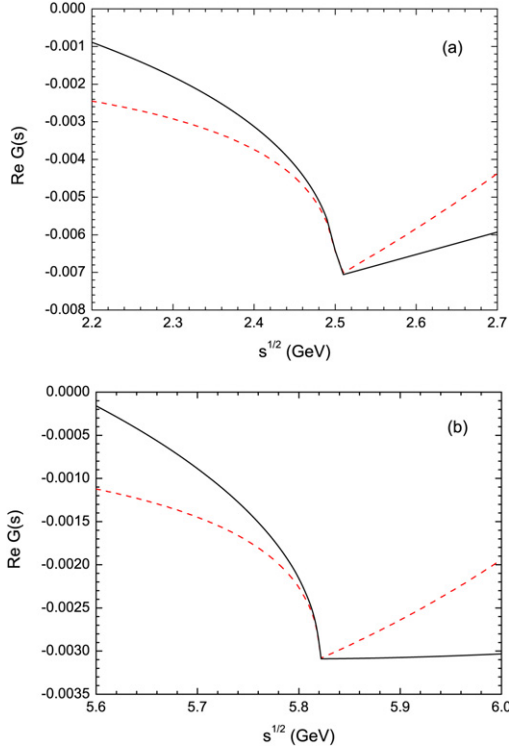


Fig. 1. The real parts of the loop integrals calculated by using the cut-off method (dashed lines) and the dispersion relation method (solid lines). (a) D^*K loop, (b) $B^*\bar{K}$ loop.

around the matching point. With the estimated $a(\mu)$ values, the unitary scattering amplitudes can be calculated.

The poles of the full scattering amplitudes in the $I = 0$, $S = 1$ channel in both the charmed sector and bottom sector are searched first. It is shown that on the first Riemann sheet of the energy plane, there is a pole located in the real axis below the lowest threshold of the coupled channels in either the charmed sector or the bottom sector. The resultant pole positions with different $a(\mu)$, which correspond to $q_{\max} = 0.6$, 0.8 and 1.0 GeV, are tabulated in Table 3, respectively. These poles are apparently associated with the D^*K bound state and the $B^*\bar{K}$ bound state, respectively. More specifically, when $a(m_D) = -0.714$, corresponding to $q_{\max} = 0.8$ GeV, the mass of the D^*K state (D_{s1}) is about 2459 MeV, which is quite consistent with the measured value of the $D_{s1}(2460)$ state [11]

$$M_{D_{s1}(2460)} = 2458.9 \pm 0.9 \text{ MeV}. \quad (6)$$

Taking into account the uncertainty of the subtraction constant, the resultant masses of the D_{s1} state and the undiscovered $B^*\bar{K}$ bound state, namely B_{s1} , are

$$\begin{aligned} M_{D_{s1}} &= 2.462 \pm 0.010 \text{ GeV}, \\ M_{B_{s1}} &= 5.778 \pm 0.007 \text{ GeV}. \end{aligned} \quad (7)$$

Table 3

Poles in the $(I, S) = (0, 1)$ case

| q_{\max} (GeV) | 0.6 | 0.8 | 1.0 |
|------------------|-------|-------|-------|
| D_{s1} (GeV) | 2.472 | 2.459 | 2.452 |
| B_{s1} (GeV) | 5.785 | 5.775 | 5.771 |

Table 4

Poles in the $(I, S) = (0, 1)$ case in the single channel approximation

| q_{\max} (GeV) | 0.6 | 0.8 | 1.0 |
|------------------|-------|-------|-------|
| D_{s1} GeV | 2.478 | 2.467 | 2.462 |
| B_{s1} GeV | 5.786 | 5.779 | 5.775 |

Table 5

Poles in the $(I, S) = (\frac{1}{2}, 0)$ case

| q_{\max} (GeV) | 0.6 | 0.8 | 1.0 |
|------------------|--------------------------------------|--------------------------------------|--------------------------------------|
| D_1 (GeV) | $2.245 - i0.106$ $2.599 - i0.043$ | $2.239 - i0.094$ $2.585 - i0.044$ | $2.236 - i0.088$ $2.578 - i0.043$ |
| B_1 (GeV) | $5.586 - i0.118$ $5.884 - i0.027$ | $5.579 - i0.108$ $5.875 - i0.025$ | $5.576 - i0.103$ $5.870 - i0.023$ |

The predicted mass of the $B^*\bar{K}$ bound state is consistent with the simple estimate of 5778 MeV in Ref. [9].

In order to show the effect of the coupled $D_s\eta$ ($B_s\eta$) channel explicitly, we also present the single D^*K ($B^*\bar{K}$) channel result in Table 4. It is shown that the single channel results are slightly larger than the coupled channel results. It implies that $D_{s1}(2460)$ (B_{s1}) can be regarded as a bound state of D^*K ($B^*\bar{K}$) with a tiny component of $D_s\eta$ ($B_s\eta$).

In the $I = 1/2$, $S = 0$ case, the poles are located on nonphysical Riemann sheets. Usually, for a certain energy if $\text{Im } p_{\text{cm}}$ is negative in all the opened channels, the pole obtained would correspond more closely with the physical one. There are two poles in the charmed (bottom) sector. The width of the lower pole is broad and the width of the higher one is relatively narrow. We tabulated these results in Table 5. In the charmed (bottom) sector, the lower pole is located on the second Riemann sheet ($\text{Im } p_{\text{cm}1} < 0$, $\text{Im } p_{\text{cm}2} > 0$, $\text{Im } p_{\text{cm}3} > 0$, where $p_{\text{cm}i}$ is the momentum of one of the interacting mesons in the center of mass frame in the i th channel) and should be associated with the $D^*\pi$ ($B^*\pi$) resonance. This state should easily decay into $D^*\pi$ ($B^*\pi$). The higher pole in the charmed (bottom) sector is found on the third Riemann sheet ($\text{Im } p_{\text{cm}1} < 0$, $\text{Im } p_{\text{cm}2} < 0$, $\text{Im } p_{\text{cm}3} > 0$) and should be associated with an “unstable” $D_s^*\bar{K}$ (B_s^*K) bound state due to its narrow width. It should be mentioned that the pole structures of 1^+ states here are very similar to those of 0^+ states [26], but are different from that of the $f_0(980)$ state where only one pole located on the second Riemann sheet and one shadow pole on the third Riemann sheet [28]. The origin of the difference comes from the fact that there are two coupled channels, i.e. the $\pi\pi$ and $K\bar{K}$ channels, in the $f_0(980)$ state case, while there are three coupled channels in the 1^+ state case.

The fact that two poles in the different Riemann sheets should be associated with two different 1^+ states in the $I = 1/2$ channel can be confirmed by checking the curve structure of

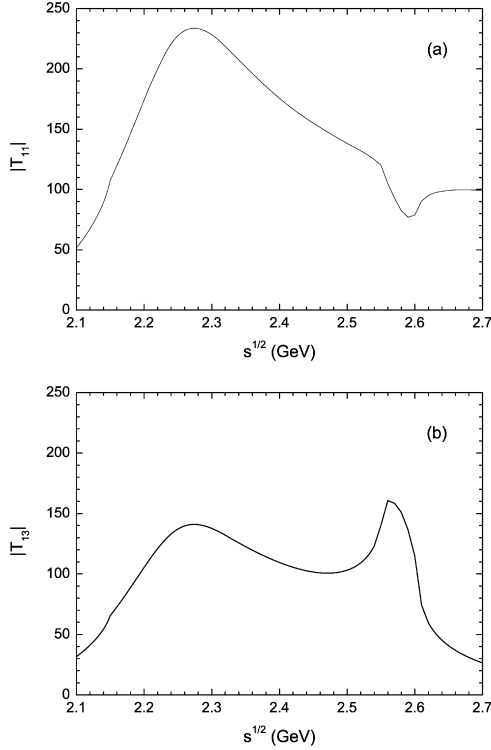


Fig. 2. The absolute values of unitary scattering amplitudes in the coupled-channel case for the $D^*\pi \rightarrow D^*\pi$ and $D_s^*\bar{K} \rightarrow D^*\pi$ processes in the $I = 1/2$ channel. (a) $D^*\pi \rightarrow D^*\pi$, (b) $D_s^*\bar{K} \rightarrow D^*\pi$.

the absolute values of the unitary scattering amplitudes in the coupled channel case, because such curve structure is closely related to the structure in the corresponding invariant mass spectrum. The absolute values of the unitary scattering amplitudes in the coupled-channel case for the $D^*\pi \rightarrow D^*\pi$ and $D_s^*\bar{K} \rightarrow D^*\pi$ processes in the $I = 1/2$ channel are plotted in Figs. 2(a) and 2(b), respectively. It is shown that there are one broad peak and one narrow dip in the $D^*\pi \rightarrow D^*\pi$ scattering amplitude and two peaks in the $D_s^*\bar{K} \rightarrow D^*\pi$ case. In the bottom sector, the curve structure of scattering amplitudes is the same and will not be demonstrated here for simplicity.

Considering the uncertainty of $a(\mu)$ in Table 5, we predict the masses and the widths of the broad D_1 and B_1 states as

$$\begin{aligned} M_{D_1} &= 2.240 \pm 0.005 \text{ GeV}, \\ \Gamma_{D_1} &= 0.194 \pm 0.019 \text{ GeV}, \\ M_{B_1} &= 5.581 \pm 0.005 \text{ GeV}, \\ \Gamma_{B_1} &= 0.220 \pm 0.015 \text{ GeV}, \end{aligned} \quad (8)$$

respectively, and the masses and the widths of the narrow D_1 and B_1 states as

$$\begin{aligned} M_{D_1} &= 2.588 \pm 0.010 \text{ GeV}, \\ \Gamma_{D_1} &= 0.087 \pm 0.001 \text{ GeV}, \\ M_{B_1} &= 5.877 \pm 0.007 \text{ GeV}, \\ \Gamma_{B_1} &= 0.050 \pm 0.003 \text{ GeV}, \end{aligned} \quad (9)$$

respectively.

Table 6
Masses of 1^1P_1 and 1^3P_1 heavy–light mesons in quark models

| | Ref. [13] | Ref. [29] | Ref. [16] |
|------------------|-----------|-----------|-----------|
| $D_1(1^1P_1)$ | 2.44 | 2.46 | 2.490 |
| $D_1(1^3P_1)$ | 2.49 | 2.47 | 2.417 |
| $D_{s1}(1^1P_1)$ | 2.53 | 2.55 | 2.605 |
| $D_{s1}(1^3P_1)$ | 2.57 | 2.55 | 2.535 |
| $B_1(1^1P_1)$ | | 5.78 | 5.742 |
| $B_1(1^3P_1)$ | | 5.78 | 5.700 |
| $B_{s1}(1^1P_1)$ | | 5.86 | 5.842 |
| $B_{s1}(1^3P_1)$ | | 5.86 | 5.805 |

These results mean that if we believe that the $D_{s0}^*(2317)$ and $D_{s1}^*(2460)$ states in the $(I, S) = (0, 1)$ channel are really dominated by the molecular state structure, the predicted two 1^+ states in the $(I, S) = (1/2, 0)$ channel should also exist. As mentioned in the introduction, the experimentally established 1^+ states $D_1(2420)$ and $D_1(2430)$ are compatible with the conventional $c\bar{q}$ interpretation. It implies that there are no experimentally established states as the candidates for the predicted $(I, S) = (1/2, 0)$ states. Why these two states have not been observed are complex? At the present time, it is not at all clear about what to expect with regards to production of these states. In fact, finding a new state does not only depend on its high production rate, but also relate to, in a large extent, the data measurement and analysis, which are usually affected by many factors, for instance the data statistics, the background, the width of the state, the complexity of the spectrum structure in the vicinity of the state, and the suitable channels for producing and detecting such a state, and etc. For instance, one of the possible reasons which makes the observation of the predicted states difficult is that the production of such states would be suppressed with respect to conventional ones. This is because: (1) The predicted two D_1 states are quasi-bound states of other two mesons. From the viewpoint of quark degrees of freedom, there should be at least four quarks in the Fock space. Therefore, the production of such states would be suppressed in comparison with producing a $c\bar{q}$ state due to the necessary creation of an additional quark–anti-quark pair. (2) The widths of predicted D_1 states are comparable with those of the corresponding conventional $c\bar{q}$ states, so that the couplings between these states to the $D^*\pi$ state would be similar with the $c\bar{q}$ states. In other words, the signals of the predicted D_1 states would be suppressed compared with those of the conventional $c\bar{q}D_1$ states in the $D^*\pi$ spectrum, and a definite observation of such states becomes difficult. It seems that an even larger data set with higher statistics and further careful data analysis, as well as theoretical study are necessary.

Moreover, it is interesting to compare our predicted states with the quark model predicted conventional $q\bar{q}$ states shown in Table 6 [13,16,29]. We find that the lowest masses of the conventional $Q\bar{s}$ states with $J^P = 1^+$ are larger than those of our quasibound D_{s1} and B_{s1} states, respectively, and the lowest masses of the conventional $Q\bar{q}$ ($q = u, d$) states with $J^P = 1^+$ are sited between the masses of our lower and higher predicted states. Hence, if one can find a state with a mass much lower

than the quark model prediction, it might be the lower state in our prediction.

3. Coupling constants and decay widths

The nature of dynamically generated states can be further studied by calculating the coupling constants between these states and the particles in the coupled channels. The coupling constants are related to the Laurent expansions of unitary scattering amplitudes around the pole [30]

$$T_{ij} = \frac{g_i g_j}{s - s_{\text{pole}}} + \gamma_0 + \gamma_1(s - s_{\text{pole}}) + \dots, \quad (10)$$

where g_i and g_j are the coupling constants of the generated state to the i th and j th channels. The product $g_i g_j$ can be obtained by calculating the residue of the unitary scattering amplitude at the pole [21]

$$g_i g_j = \lim_{s \rightarrow s_{\text{pole}}} (s - s_{\text{pole}}) T_{ij}. \quad (11)$$

As a typical example, we calculate the coupling constants for the $D_{s1}(2460)$ state with a subtraction constant which corresponds to $q_{\text{max}} = 0.8$ GeV, because under this condition the empirical mass of $D_{s1}(2460)$ can be excellently reproduced. The resultant coupling constants are tabulated in Table 7 for the states with $I = 0$ and Table 8 for the states with $I = 1/2$.

Comparing the coupling constants in Tables 7 and 8 with those of the generated scalar states in Tables 6 and 7 in Ref. [26], one finds that the values of corresponding coupling constants are close. This manifests the heavy flavor spin symmetry [31] respected in the leading order heavy chiral Lagrangian [27]. In Table 7, the data also show that g_1 is larger than g_2 in the charmed (bottom) sector. This indicates that the coupling between the $D_{s1}(B_{s1})$ state and the states in the $D^*K(B^*\bar{K})$ channel is larger than that between the $D_{s1}(B_{s1})$ state and the states in the $D_s^*\eta(B_s^*\eta)$ channel. It also reflects the fact that the generated state is a $D^*K(B^*\bar{K})$ bound state. In Table 8, the largest coupling constant $|g_1|$ for the lower state is associated with the $D^*\pi(B^*\pi)$ channel and the largest coupling constant $|g_3|$ for the higher state is connected with the $D_s^*\bar{K}(B_s^*K)$ channel. This is consistent with our finding in the

Table 7
Coupling constants of the generated D_{s1} and B_{s1} states to relevant coupled channels. In this case, g_1 and g_2 are real. All units are in GeV

| | Masses | $ g_1 $ | $ g_2 $ |
|----------|--------|---------|---------|
| D_{s1} | 2.459 | 10.762 | 6.170 |
| B_{s1} | 5.775 | 23.572 | 13.326 |

Table 8
Coupling constants of the generated D_1 and B_1 states to relevant coupled channels. All units are in GeV

| | Poles | g_1 | $ g_1 $ | g_2 | $ g_2 $ | g_3 | $ g_3 $ |
|-------|------------------|--------------------|---------|--------------------|---------|--------------------|---------|
| D_1 | $2.239 - i0.094$ | $8.157 + i5.135$ | 9.639 | $-0.202 + i0.059$ | 0.211 | $4.919 + i3.053$ | 5.790 |
| D_1 | $2.585 - i0.044$ | $0.145 + i3.306$ | 3.309 | $-6.893 - i2.237$ | 7.247 | $-11.060 + i1.165$ | 11.121 |
| B_1 | $5.579 - i0.108$ | $21.439 + i11.861$ | 24.502 | $-2.222 - i0.752$ | 2.346 | $13.517 + i6.906$ | 15.179 |
| B_1 | $5.875 - i0.025$ | $0.295 + i6.619$ | 6.626 | $-14.553 - i4.892$ | 15.353 | $-24.759 - i0.874$ | 24.775 |

pole analysis, namely the lower state is a $D^*\pi(B^*\pi)$ resonance and the higher state associates with a $D_s^*\bar{K}(B_s^*K)$ quasi-bound state.

The coupling constants also show that the largest component of the lower D_1 state is $D^*\pi$ whose quark contents are $c\bar{n}n\bar{n}$, where n denotes the u or d quark, and the largest component of the higher D_1 state is $D_s^*\bar{K}$ whose quark contents are $c\bar{s}s\bar{s}$. On the other hand, the $D_{s1}(2460)$ state, in principle, is a D^*K bound state, and consequently, the dominant quark contents of this state are $c\bar{n}n\bar{s}$. Thus, from the quark contents of these states, one can expect that the mass of D_{s1} should be a value between the masses of the two D_1 states. The same qualitative statement can be applied to the bottom sector.

Furthermore, the dynamic nature of a state can be characterized by its decay properties. Since the quark contents of predicted molecular states are different from those of conventional $q\bar{q}$ states, their decay properties are expected to be different.

In order to estimate the order of magnitude of the decay width of $D_{s1}(2460)$, we calculate the decay widths of the isospin symmetry violating decay processes $D_{s1}(2460)^+ \rightarrow D^{*+}\pi^0$ and $B_{s1}(5775)^0 \rightarrow B^{*0}\pi^0$ can be estimated through π^0 - η mixing [32] shown in Fig. 3. By using the formula

$$\Gamma = \frac{p_{\text{cm}}}{8\pi M^2} \sum_{\lambda} \sum_{\lambda'} \left| \frac{g_2 t_{\pi\eta} \epsilon^{\lambda}(p) \cdot \epsilon^{\lambda'}(p_1)}{m_{\pi^0}^2 - m_{\eta}^2} \right|^2, \quad (12)$$

where M is the mass of the initial meson, p_{cm} denotes the three-momentum in the center of mass frame, $\epsilon^{\lambda}(p)$ and $\epsilon^{\lambda'}(p_1)$ represent the polarization vectors of the $D_{s1}(2460)$ ($B_{s1}(5775)$) and D^* (B^*) states, respectively, and $\sum_{\lambda} \sum_{\lambda'}$ describes the sum over the final states and the average over the initial states. By using the π^0 - η mixing amplitude $t_{\pi\eta} = -0.003$ GeV obtained from the Dashen's theorem [33], we get the decay widths

$$\begin{aligned} \Gamma(D_{s1}(2460)^+ \rightarrow D_s^{*+}\pi^0) &= 11.41 \text{ keV}, \\ \Gamma(B_{s1}(5775)^0 \rightarrow B_s^{*0}\pi^0) &= 10.36 \text{ keV}. \end{aligned} \quad (13)$$

It should be mentioned that, the explicit isospin breaking term is

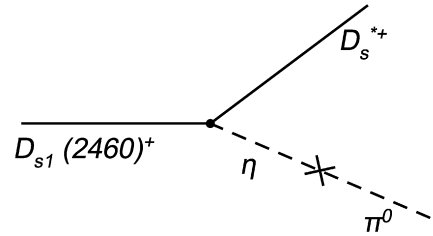


Fig. 3. Isospin symmetry violating decay process $D_{s1}(2460)^+ \rightarrow D_s^{*+}\pi^0$ via π^0 - η mixing.

not the only source of isospin breaking, the mass difference of isospin multiplets has already generated such a breaking. Thus, the given result can only serve an estimate of the order of magnitudes of the widths.

The decay properties of predicted $D_1 (B_1)$ state can also be briefly estimated. For the higher $D_1 (B_1)$ states, it can strongly decay into the two opened channels: $D^*\pi$ and $D^*\eta (B^*\pi$ and $B^*\eta)$. Although the channel with η have much smaller phase space than that with π , due to the relatively larger contribution from hidden strangeness, which can be seen from Table 8, the branching fraction of the $D_1 (B_1)$ state decaying into the final state with η is comparable with or even larger than that with π . The ratio of these two branching fractions can roughly be estimated by using corresponding coupling constants given in Table 8

$$\begin{aligned} R_{\eta/\pi^0}(D_1) &\equiv \frac{\Gamma(D_1 \rightarrow D^*\eta)}{\Gamma(D_1 \rightarrow D^*\pi)} \simeq 1.57, \\ R_{\eta/\pi^0}(B_1) &\equiv \frac{\Gamma(B_1 \rightarrow B^*\eta)}{\Gamma(B_1 \rightarrow B^*\pi)} \simeq 0.50. \end{aligned} \quad (14)$$

As to the conventional $D_1 (B_1)$ state which has a mass larger than the $D^*\eta (B^*\eta)$ threshold, the branching fraction of decaying into $D^*\eta (B^*\eta)$ would be much smaller than that into $D^*\pi (B^*\pi)$ due to both OZI suppression [34] and phase space suppression. Thus, it would be easy to distinguish this state from the higher $D_1 (B_1)$ state by measuring the ratio defined in Eq. (14). For the lower $D_1 (B_1)$ state predicted here, it has only one opened channel $D^*\pi (B^*\pi)$. So it would be difficult to distinguish the lower state from the conventional $D_1 (B_1)$ state with similar mass and width by using strong decay properties. Yet, the radiative decays of such states might be different. The concrete consequences should be investigated in future.

4. Conclusion

We study the dynamically generated axial heavy mesons which have the same quantum numbers of the conventional $c\bar{s}$ and $c\bar{q}$ states in the $(I, S) = (0, 1)$, $(I, S) = (1/2, 0)$ systems in the framework of coupled-channel HChUA. In the $(I, S) = (0, 1)$ and $J^P = 1^+$ system, there are two coupled channels: D^*K and $D_s^*\eta$ for the charmed sector and $B^*\bar{K}$ and $B_s^*\eta$ for the bottom sector, respectively. In the coupled channel calculation, the channels with a light vector meson and a heavy pseudoscalar meson are not considered due to their less importance.

By searching for the pole of the unitary coupled-channel scattering amplitude on appropriate Riemann sheets of the energy plane, we find a state with mass of 2.462 ± 0.010 GeV in the $(I, S) = (0, 1)$ system. This state should be a D^*K bound state with a tiny $D_s^*\eta$ component. We would interpret it as the recently observed charmed meson $D_{s1}(2460)$. In the same way, we predict a $B^*\bar{K}$ bound state with mass of 5.778 ± 0.007 GeV in the bottom sector. In the $(I, S) = (1/2, 0)$, $J^P = 1^+$ system, there are three coupled channels: $D^*\pi$, $D^*\eta$ and $D_s^*\bar{K}$ in the charmed sector and $B^*\pi$, $B^*\eta$ and B_s^*K in the bottom sector, respectively. We find two poles in the nonphysical Riemann

sheets in both the charmed and bottom sectors. In the charmed (bottom) sector, the lower pole is located at $(2.240 \pm 0.005 - i0.097 \pm 0.009)$ GeV ($(5.581 \pm 0.005 - i0.110 \pm 0.007)$ GeV). The state associated with this pole will strongly decay to $D^*\pi (B^*\pi)$ and have the largest coupling with the decayed particles. Therefore, this pole should be associated with the $D^*\pi (B^*\pi)$ resonance. The higher pole is positioned at $(2.588 \pm 0.010 - i0.043 \pm 0.001)$ GeV ($(5.877 \pm 0.007 - i0.025 \pm 0.002)$ GeV). The state associated with this pole has two decay channels $D^*\pi$ and $D^*\eta (B^*\pi$ and $B^*\eta)$ and has the largest coupling with decayed particles in the $D_s^*\bar{K} (B_s^*K)$ channel. Thus, this pole should be associated with a quasi-bound state of $D_s^*\bar{K} (B_s^*K)$. If one believes that the corresponding states in the $(I, S) = (0, 1)$ and $(I, S) = (1/2, 0)$ systems have similar S wave molecular state structures, the two predicted states should exist. The estimated order of magnitudes for the widths of the $D_{s1}(2460)^+$ and $B_{s1}(5775)^0$ states is about 10 keV. The decay properties of predicted $D_1 (B_1)$ states are also briefly discussed. Study the channels where the final states include $D^*\eta$ and $D^*\pi (B^*\eta$ and $B^*\pi)$ would be helpful to find predicted $D_1 (B_1)$ states.

Acknowledgements

We sincerely thank Prof. B.S. Zou for valuable discussion. We thank G. Rupp for helpful comments on their work and pointing out a typographic error in the previous version of this Letter. This work is partially supported by the NSFC grant Nos. 90103020, 10475089, 10435080, 10447130, CAS Knowledge Innovation Key-Project grant No. KJJCX2SWN02 and Key Knowledge Innovation Project of IHEP, CAS (U529).

References

- [1] BABAR Collaboration, B. Aubert, et al., Phys. Rev. Lett. 90 (2003) 242001; CLEO Collaboration, D. Besson, et al., Phys. Rev. D 68 (2003) 032002; Belle Collaboration, P. Krokovny, et al., Phys. Rev. Lett. 91 (2003) 262002; Belle Collaboration, Y. Mikami, et al., Phys. Rev. Lett. 92 (2004) 012002; E. Vaandering, in: Proceedings for the XXXIXth Rencontres de Moriond (QCD and High Energy Hadronic Interactions), March 28–April 4, 2004, La Thuile, Italy, hep-ex/0406044; BABAR Collaboration, B. Aubert, et al., in: 32nd International Conference on High-Energy Physics (ICHEP 04), August 2004, Beijing, China, hep-ex/0408067.
- [2] S. Godfrey, Phys. Lett. B 568 (2003) 254.
- [3] E.S. Swanson, Phys. Rep. 429 (2006) 243; J.L. Rosner, hep-ph/0609195.
- [4] W.A. Bardeen, E.J. Eichten, C.T. Hill, Phys. Rev. D 68 (2003) 054024; P. Colangelo, F. De Fazio, Phys. Lett. B 570 (2003) 180; E. van Beveren, G. Rupp, Phys. Rev. Lett. 91 (2003) 012003; E. van Beveren, G. Rupp, Eur. Phys. J. C 32 (2004) 493; Y.-B. Dai, C.-S. Huang, C. Liu, S.-L. Zhu, Phys. Rev. D 68 (2003) 114011; Fayyazuddin, Riazuddin, Phys. Rev. D 69 (2004) 114008; M.A. Nowak, M. Rho, I. Zahed, Acta Phys. Pol. B 35 (2004) 2377; P. Colangelo, F. De Fazio, A. Ozpineci, Phys. Rev. D 72 (2005) 074004; X.-H. Guo, H.-W. Ke, X.-Q. Li, X. Liu, S.-M. Zhao, hep-ph/0510146; T. Matsuki, T. Morii, K. Sudoh, hep-ph/0605019; J. Lu, W.-Z. Deng, X.-L. Chen, S.-L. Zhu, Phys. Rev. D 73 (2003) 054012; O. Lakhina, E.S. Swanson, hep-ph/0608011.

- [5] H.-Y. Cheng, W.-S. Hou, Phys. Lett. B 566 (2003) 193;
Y.-Q. Chen, X.-Q. Li, Phys. Rev. Lett. 93 (2004) 232001;
H. Kim, Y. Oh, Phys. Rev. D 72 (2005) 074012;
M. Nielsen, R.D. Matheus, F.S. Navarra, M.E. Bracco, A. Lozea, in: Workshop on Light-Cone QCD and Nonperturbative Hadron Physics 2005 (LC2005), July 2005, Cairns, Australia, hep-ph/0509131;
P. Bicudo, Phys. Rev. D 74 (2006) 036008;
K. Terasaki, in: Workshop on Resonances in QCD, July 2005, Trento, Italy, hep-ph/0512285;
Z.-G. Wang, S.-L. Wan, Nucl. Phys. A 778 (2006) 22.
- [6] A.P. Szczepaniak, Phys. Lett. B 567 (2003) 23;
T. Barnes, F.E. Close, H.J. Lipkin, Phys. Rev. D 68 (2003) 054006;
Y.-J. Zhang, H.-C. Chiang, P.-N. Shen, B.-S. Zou, Phys. Rev. D 74 (2006) 014013.
- [7] E.E. Kolomeitsev, M.F.M. Lutz, Phys. Lett. B 582 (2004) 39.
- [8] J. Hofmann, M.F.M. Lutz, Nucl. Phys. A 733 (2004) 142.
- [9] J.L. Rosner, Phys. Rev. D 74 (2006) 076006.
- [10] Z.-G. Wang, S.-L. Wan, Phys. Rev. D 73 (2006) 094020;
T.E. Browder, S. Pakvasa, A.A. Petrov, Phys. Lett. B 578 (2004) 365;
J. Vijande, F. Fernández, A. Valcarce, Phys. Rev. D 73 (2006) 034002.
- [11] Particle Data Group, W.-M. Yao, et al., J. Phys. G 33 (2006) 1.
- [12] Belle Collaboration, K. Abe, et al., Phys. Rev. D 69 (2004) 112002.
- [13] S. Godfrey, N. Isgur, Phys. Rev. D 32 (1985) 189.
- [14] CLEO Collaboration, T. Bergfeld, et al., Phys. Lett. B 340 (1994) 194.
- [15] F.E. Close, E.S. Swanson, Phys. Rev. D 72 (2005) 094004.
- [16] M. Di Pierro, E. Eichten, Phys. Rev. D 64 (2001) 114004.
- [17] S. Godfrey, Phys. Rev. D 72 (2005) 054029.
- [18] N. Kaiser, T. Waas, W. Weise, Nucl. Phys. A 612 (1997) 297;
E. Oset, A. Ramos, Nucl. Phys. A 635 (1998) 99;
B. Krippa, Phys. Rev. C 58 (1998) 1333;
B. Krippa, J.T. Londergan, Phys. Rev. C 58 (1998) 1634.
- [19] J.A. Oller, E. Oset, Nucl. Phys. A 620 (1997) 438;
J.A. Oller, E. Oset, Nucl. Phys. A 652 (1999) 407, Erratum.
- [20] J.A. Oller, E. Oset, J.R. Peláez, Phys. Rev. Lett. 80 (1998) 3452;
J.A. Oller, E. Oset, J.R. Peláez, Phys. Rev. D 59 (1999) 074001.
- [21] J.A. Oller, E. Oset, Phys. Rev. D 60 (1999) 074023.
- [22] N. Kaiser, Eur. Phys. J. A 3 (1998) 307;
J. Nieves, E. Ruiz Arriola, Phys. Lett. B 455 (1999) 30;
V.E. Markushin, Eur. Phys. J. A 8 (2000) 389.
- [23] U.-G. Meißner, J.A. Oller, Nucl. Phys. A 673 (2000) 311;
J.A. Oller, Phys. Lett. B 500 (2001) 263.
- [24] L. Roca, E. Oset, J. Singh, Phys. Rev. D 72 (2005) 014002.
- [25] F.-K. Guo, R.-G. Ping, P.-N. Shen, H.-C. Chiang, B.-S. Zou, Nucl. Phys. A 773 (2006) 78.
- [26] F.-K. Guo, P.-N. Shen, H.-C. Chiang, R.-G. Ping, B.-S. Zou, Phys. Lett. B 641 (2006) 278.
- [27] G. Burdman, J.F. Donoghue, Phys. Lett. B 280 (1992) 287;
M.B. Wise, Phys. Rev. D 45 (1992) 2188;
T.-M. Yan, H.-Y. Cheng, C.-Y. Cheung, G.-L. Lin, Y.C. Lin, H.-L. Yu, Phys. Rev. D 46 (1992) 1148;
R. Casalbuoni, A. Deandrea, N. Di Bartolomeo, R. Gatto, F. Feruglio, G. Nardulli, Phys. Rep. 281 (1997) 145.
- [28] B.S. Zou, D.V. Bugg, Phys. Rev. D 48 (1993) R3948.
- [29] S. Godfrey, R. Kokoski, Phys. Rev. D 43 (1991) 1679.
- [30] J.A. Oller, Phys. Rev. D 71 (2005) 054030.
- [31] M. Neubert, Phys. Rep. 245 (1994) 259.
- [32] P. Cho, W.B. Wise, Phys. Rev. D 49 (1994) 6228.
- [33] R. Dashen, Phys. Rev. 183 (1969) 1245.
- [34] S. Okubo, Phys. Lett. 5 (1963) 165;
G. Zweig, CERN preprints TH-401, TH-412 (1964);
J. Iizuka, Prog. Theor. Phys. Suppl. 38 (1966) 21.